New Insights into Evaluation of Kinetic Parameters for Potentiostatic Metal Deposition with Underpotential and Overpotential Deposition Processes

Manuel Palomar-Pardavé

Departamento de Materiales, Universidad Autónoma Metropolitana-Azcapotzalco, A.P. 16-306, C.P. 02000 México, D.F., México

Ignacio González and Nikola Batina*

Departamento de Química, Universidad Autónoma Metropolitana-Iztapalapa, A.P. 55-534, 09340 México, D.F., México

Received: September 9, 1999; In Final Form: January 10, 2000

Kinetics of copper deposition onto an Au(111) surface from sulfuric acid electrolyte, was evaluated using potentiostatic current transients. Measurements were conducted employing a new and nontraditional method, with gold electrode completely free from copper deposit at the beginning of the potential step (i.e., deposition process). The current transients obtained clearly show partial contribution from copper underpotential deposition (UPD) and copper overpotential deposition (OPD) processes. Quantitative evaluation of experimental transients was performed with the recently developed method for theoretical transient computer simulation. Detailed analysis of the kinetic parameters shows that copper UPD could be characterized as a two-dimensional nucleation and growth limited by the lattice incorporation (2D-LI) process and copper OPD as a three-dimensional nucleation process limited by diffusion-controlled growth (3D-DC). The UPD seems to be an inevitable part of the deposition process and takes place prior to OPD, regardless of the potential applied. Therefore, UPD should be treated as an early stage of the deposition process. Furthermore, our results show that the kinetics differs depending on whether deposition is initiated from a clean, bare Au(111) surface or from a gold surface already coated with a copper UPD adlayer. This indicates the role of the UPD process and the UPD adlayer on the course of OPD. Differences observed in deposition kinetics between electrolytic baths at pH 2 and 4 were likely due to adsorption of different sulfate species (sulfate or bisulfate anions) on the copper-deposit-modified Au(111) substrate (UPD, epitaxial monolayer) or bulk deposit adlayer (OPD).

1. Introduction

Copper deposition is a crucial process nowadays in industrial technology, especially in the area of electronics. It has been studied intensively on a variety of substrates from different electrolytic baths. Many newly developed techniques and methods have been successfully tested for such copper deposition studies.

Copper deposition onto a single-crystal, gold electrode is a frequently used model system for elucidating detailed mechanisms of the metal deposition process onto foreign metal substrates. It is well established that, on single-crystal electrodes, copper deposition proceeds via two, well-defined stages: underpotential deposition (UPD), at potentials before reaching the Nernst equilibrium potential, and overpotential deposition (OPD), also known as bulk deposition, in a potential region above the Nernst equilibrium potential. Many aspects of both UPD and OPD processes have been described in great detail, including electrodeposition onto the Au(111) surface, the structure of the copper−UPD adlayer and its mechanism of formation, and the influence of different (coadsorbed) anions on UPD adlayer formation.[1,2] Recent progress in the field has made use of modern, in situ techniques for structural characterization such as STM,[3−13] in situ X-ray measurements,[14−19] in situ electrochemical quartz crystal microbalance studies,[20,21] and updated electrochemical studies.[22−25]

Studies of copper OPD onto Au(111) have focused on determining deposit morphology, characterizing kinetics of the electronucleation process, and examining how different molecular additives influence the course of the deposition process.[7,26−45] The most recent papers are related to the SPM techniques, which have become a favorite tool for metal deposition investigation.

The electrocrystallization mechanism and copper deposition growth kinetics on the Au(111) surface are not as well characterized as the structure of the UPD adlayer.[34,46−47] In recent reports, the kinetics of copper electrocrystallization onto Au(111) for both UPD and OPD, were defined by treating UPD and OPD as two independent processes. Scant information exists to describe the influence of the UPD process on the OPD reaction. If copper UPD is considered an early stage of the copper deposition process onto the Au(111) surface, determination of the UPD−OPD link becomes especially important for comprehension of overall deposition mechanisms. UPD is a surface phenomenon, depending on the substrate structure, substrate physical−chemical characteristics, and deposit (adatom)−substrate interactions. As a result of the UPD process, which takes place at more positive potentials than the deposition equilibrium potential (Nernst potential), the electrode surface is partially or completely (up to an epitaxial monolayer) covered by a metal deposit. The structure and amount of adatoms on

* To whom correspondence should be addressed. Fax: (52)(5) 804-4666. E-mail: bani@xanum.uam.mx.

10.1021/jp9931861 CCC: $19.00 © 2000 American Chemical Society
Published on Web 03/22/2000

the UPD layer are strongly affected by coadsorbed anions as described in various studies dealing with the influence of anions on copper UPD on Au(111).[1−4,7,17,22−25]

The OPD process is determined by electrode potential (overpotential), deposit growth kinetics and mechanism (2D or 3D), electroactive species concentration, and deposit−substrate and deposit−deposit interactions. OPD takes place at more negative potentials than the Nernst equilibrium potential. Thus, it is well established that during the scan from positive potentials, where no copper deposition occurs, in the negative direction, UPD and OPD processes take place consecutively, one after the other. In effect, the OPD process takes place on an electrode surface, which has already been modified by the UPD adlayer, rather than on the bare electrode substrate. UPD can, thereby, be considered as deposition of copper adatoms onto the gold substrate, while OPD involves copper adatom deposition on the gold substrate modified by the copper monolayer, formed during the copper UPD process.[3,4,9] Kolb et al.,[34,46−47] studied the kinetics of the copper UPD on the bare Au(111) surface and copper OPD onto the Au(111) surface modified by a copper UPD adlayer as independent events.

Copper OPD onto bare Au(111), involving copper UPD as an integral, early-stage process, has yet to be described. The influence of UPD on the kinetics and mechanisms of copper OPD, therefore, remains obscure. Many interesting questions arise when considering the UPD adlayer as a precursor for a further deposition process. Another issue is recognition of partial contributions from UPD and OPD processes, within the single current transient as a typical measure (cumulative response) of the kinetic behavior for the deposition process. Furthermore, the relationship of metal deposition kinetics to the pH of the electrolytic bath is an important issue to be determined as well. Since during the UPD/OPD process the electrode surface (top outmost layer) is covered by different materials, its reactivity with solution anions could be altered significantly by changes in pH.

We studied copper OPD deposition onto Au(111) substrate from 0.1 M H_2SO_4 solution to address these issues. Current transients for the copper OPD process were recorded with two different starting potentials with the gold electrode surface free of copper deposit and with a copper UPD deposit-covered electrode surface. Thus, depending on the chosen starting potential, the formation of copper OPD deposit was initiated on either the bare Au(111) surface or the copper UPD modified Au(111) surface. In both cases, the two-dimensional copper UPD process is an inevitable phase, which is always involved in a deposition process as an early stage of OPD. The copper OPD always proceeds at the gold electrode surface which is already modified by the copper UPD adlayer. To interpret experimental current transients for UPD/OPD processes, we applied a newly developed method[48] capable of handling complexly shaped current transients and taking into account the contributions from all processes involved in deposition. Besides determining standard kinetic parameters, such as nucleation rates (A), the number density of active sites (N_o), and the number density of formed nuclei (N_s), for characterization of electrocrystallization and deposit growth, this method also allows us to estimate the influence of the UPD process on the copper OPD deposition.

Our study demonstrates a convenient methodology for recognition and quantitative estimation of kinetic parameters for the OPD deposition process that involves a UPD as a preliminary reaction step.

2. Experimental Section

2.1. Chemicals and Solutions. $CuSO_4$ and KOH used were ultrapure grade from Merck. All solutions were prepared with ultrapure water (Millipore Milli-Q). N_2 gas, 99.99% pure, was purchased from Praxair. All Cu(II) aqueous sulfuric solutions (concentrated 1 mM) have been prepared with 0.1 M H_2SO_4 (pH 1) solution. Acidity in pH 4 solutions was adjusted by KOH solution.

2.2. Electrochemical Setup. Cyclic voltammetry and chronoamperometry were employed to study the copper electrodeposition over a Au(111) substrate from an electrolytic bath containing 1 mM Cu(II) and 0.1 M H_2SO_4 (pH 1 and 4). Electrochemical experiments were carried out in a conventional three-electrode cell system using a Au(111) working electrode with a 0.20 cm^2 surface area, a platinum wire counter electrode, and a saturated mercury sulfate reference electrode, Hg/Hg_2SO_4, K_2SO_4 (SMSE). All potentials are quoted vs the SMSE reference electrode. Prior to electrochemical experiments, solutions were carefully deareated for 30 min using clean nitrogen gas. Potentials were controlled by a PAR 273 (USA) potentiostat coupled to a computer with a commercial "M-270" (PAR) software package for experimental control and data acquisition. To avoid uncontrolled copper deposition at the open circuit potential, the working electrode was constantly maintained under the potential control, from initial contact with solution. Cyclic voltammetry was performed in the potential range between −0.050 and −0.550 V vs SMSE, with a scan rate of 15 mV/s. Scans were always initiated at −0.050 V, after 15 s of conditioning at this potential. Although several consecutive scans show the same voltammograms, only the first scans are presented.

2.3. Substrate. The Au(111) substrate, used as a working electrode, consisted of a 200 nm thick gold film evaporated onto a special heat-resistive glass (BerlinerGlas KG), with a 2 nm thick Cr adhesive undercoating layer. Gold-coated glass was cut to the desired shape using a diamond saw, and the electrode was carefully rinsed with ultrapure water. To obtain large terraces with (111) orientation in the subsequent processes, sample was annealed in a hydrogen air flame at orange/yellow heat for 2−3 min. This annealing treatment was previously demonstrated to produce a quality (111) surface, comparable to a massive (111) single crystal.[35] After resting and cooling in a hydrogen flux for 20−30 s, the sample was transferred to the electrochemical cell under potential control.

2.4. Potentiostatic Current Transient Measurements. To estimate kinetic parameters of copper deposition onto the Au(111) electrode, a set of potentiostatic current transients was obtained at different deposition potentials. Measurements were performed by a single-potential-step method (standard chronoamperometric technique), which essentially involves stepping the potential from the initial value, where no deposition occurs, to the final potential, in the region where deposition takes place. To resolve the possible influence of the copper UPD process on kinetic characteristics of copper bulk deposition (OPD), chronoamperometric measurements were performed with two different values for the initial potentials. In the first set of experiments the initial potential was placed in the potential region where no deposition occurs, at all. In the second case, the initial potential was chosen to be in the final part of the copper UPD range, such that the OPD deposit was grown onto the UPD adlayer. Between the subsequent potential steps, the electrode surface was always cleaned of all copper deposit by applying positive potential where copper deposition does not take place.

2.5. Quantitative Interpretation of Current Potential Measurements. Results of chronoamperometric measurements to evaluate the kinetics and mechanism of copper electrocrystallization onto the Au(111) electrode surface were quantitatively evaluated using a homemade software package developed for the PC computer system. Regardless of the experimental procedure during the chronoamperometric measurements, all data were processed identically, through several distinct steps. The set of the obtained potentiostatic $I-t$ curves was analyzed to estimate how many and which mechanisms are involved in the electrocrystallization process. The next step was to graph experimentally obtained data in nondimensional plots to determine the mechanisms involved with more accuracy. For these plots, complete or only the most revealing portion of the $I-t$ curves was considered. On the basis of this information, a reasonable input for initiating calculation for theoretical $I-t$ transients was defined. All processes involved in the adsorption, electrocrystallization, and the deposit growth, proceeded simultaneously during simulation, without input set restrictions. A theoretical transient with a best fit (nonlinear fitting procedure) to experimental data for all processes involved during the transient recording is offered as a final output in a last part of the simulation process. Major kinetic parameters for each process involved in the deposition reaction, as well as the relationship between different processes (mechanisms), were obtained from this theoretical transient (integral).

3. Results and Discussion

Copper deposition onto the Au(111) surface was carried out from 1 mM Cu^{2+}/0.1 M H_2SO_4 solutions of pH 1 and 4. According to a previous report,[47] the kinetics of copper OPD onto Au(111) depends on the electrolyte pH value. Kolb and coauthors[47] studied copper deposition onto Au(111) from sulfate solutions with pH varied from 2 to 4, and observed significant changes in the shape of the current transients, indicating different copper deposition mechanisms at different pH values. Transients with a well-defined current maximum observed at pH 4 were associated with a 3D progressive electrocrystallization. At pH below 4 (i.e., pH 2), nucleation changed from a 3D progressive to 3D instantaneous process. The change in nucleation mechanism is caused by a decrease in nucleation sites at the electrode surface in response to the strength of the anion adsorption, since sulfate at pH higher than 2 becomes bisulfate at a lower pH. Strongly adsorbed bisulfate supposedly hinders the Cu nucleation sites. Evaluation of kinetic parameters was based on the set of the potentiostatic current transients, which were recorded at a stepping potential from 52 mV vs copper reference electrode toward more negative potentials, in the OPD potential region. Since the starting potential of 52 mV is just before the OPD process begins and in the potential range where UPD is almost completed, these results described copper deposition onto the Au(111) electrode which had already been modified by a copper adlayer (most probably an epitaxial monolayer of copper adatoms on Au(111).[3,4,9] This means that nucleation of copper adatoms during the OPD process actually takes place at the copper monolayer that was previously adsorbed at the Au(111) electrode surface, during the UPD process. The current transients obtained in this particular experiment were of the simple shape, with a single current maximum related to the 3D-OPD process.

As discussed above, in our experiment, current transient measurements were performed from two starting potentials. Initiation was either in the region free of copper deposit (bare gold electrode surface) or where the gold electrode was already modified with a copper UPD adlayer (such as described by Kolb et al.[47]). The initial electrode surface conditions for the OPD process were, thus, a function of the starting potential applied during potential step measurements. Our current transients for copper deposition onto the bare Au(111) surface were very complex, with two or more current maxima. However, using a new method for evaluation of current transients with several nucleation (deposition) processes, we were able to distinguish and characterize the UPD and OPD processes.

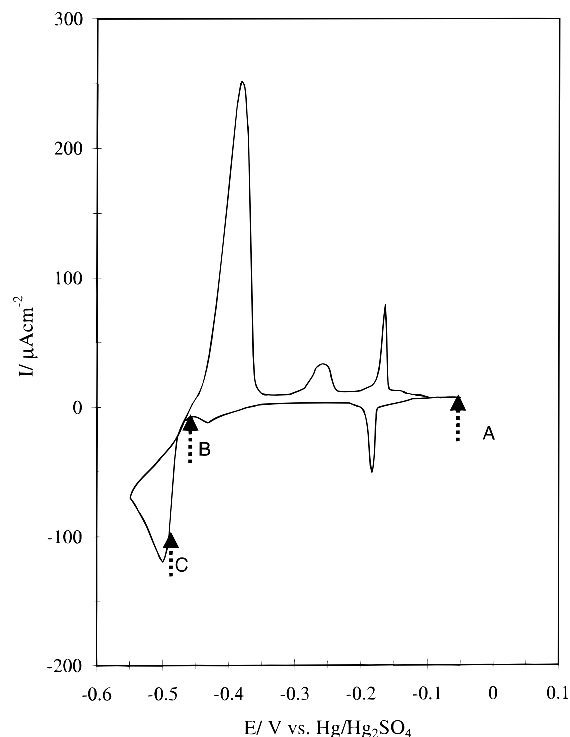

Figure 1. Cyclic voltammogram for copper deposition onto Au(111) from 1 mM $CuSO_4$ + 0.1 M H_2SO_4 (pH 4). The potential scan starts at −0.05 V, with a scanning rate of 15 mV/s. The voltammogram shows the copper UPD ($E > -0.463$ V) and OPD ($E < -0.463$ V) deposition regions. A, B, and C correspond to different initial (A and B) and final (C) potentials applied during the current transient measurements.

3.1. Copper Deposition from 0.1 M H_2SO_4 (pH 4). Figure 1 shows a typical voltammogram obtained for copper deposition onto the Au(111) surface from 0.1 M H_2SO_4, pH 4. The potential scan was started from −0.05 V, run toward the negative potential up to −0.55 V, and then reversed to the starting point. The voltammogram shows the copper UPD and OPD processes. To clearly define the beginning of the copper OPD process, the Nernst equilibrium potential of the copper deposition process for our experimental conditions was estimated: −0.463 V.[49] Therefore, copper deposition, taking place at potentials more positive than −0.463 V, was defined as occurring by the UPD process. In this region, two characteristic deposition peaks at −0.180 and −0.420 V and two dissolution peaks at −0.250 and −0.150 V were observed. Large voltammetric peaks seen at −0.500 V (cathodic scan) and −0.365 V (anodic scan) were related to copper OPD deposition and dissolution processes, respectively.

The peak number, shape, potential, and magnitude observed for both deposition processes (UPD and OPD) in our voltammogram agreed perfectly with previously published data.[2−4,6−7] It was recently established that copper is randomly adsorbed at potentials more positive than the first deposition UPD peak (−0.180 V). This is followed by formation of a $(\sqrt{3}\times\sqrt{3})R30°$ honeycomb adlayer consisting of copper and coadsorbed sulfate or bisulfate in the potential region between two UPD peaks,

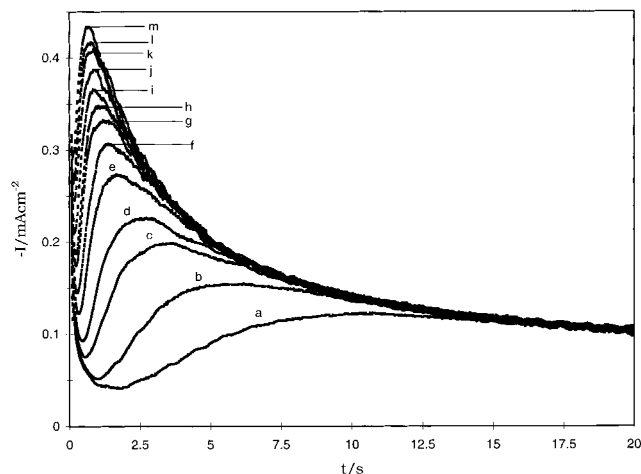

Figure 2. Set of experimental current transients recorded for copper OPD onto Au(111) previously covered by a Cu UPD adlayer, from 1 mM $CuSO_4$ + 0.1 M H_2SO_4 (pH 4), at different electrode potentials: (a) −0.473 V, (b) −0.474 V, (c) −0.476 V, (d) −0.477 V, (e) −0.479 V, (f) −0.481 V, (g) −0.482 V, (h) −0.483 V, (i) −0.484 V, (j) −0.485 V, (k) −0.486 V, (l) −0.487 V, and (m) −0.488 V. The starting potential was always −0.463 V (marked as B in Figure 1).

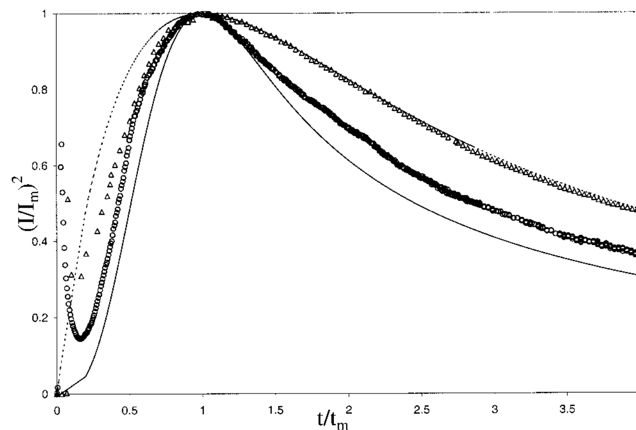

Figure 3. Comparison between experimental (points) and theoretical (lines) current transients for copper OPD onto Au(111) previously covered by a Cu UPD adlayer from 1 mM $CuSO_4$ + 0.1 M H_2SO_4 (pH 4) solution, presented in the nondimensional $(I/I_m)^2$ vs t/t_m plot. Theoretical transients for instantaneous (dashed line) and progressive (full line) nucleation were calculated according to the Scharifker model.[50] The experimental transients were recorded at different electrode potentials, (○) −0.477 V and (Δ) −0.489 V, under the same conditions as in Figure 2.

and formation of a pseudomorphic (1×1) adlayer of the copper monolayer on Au(111) at potentials more negative than the second UPD peak (−0.420 V).[3,4,9,15−17,20]

To characterize kinetic parameters of the copper deposition onto the bare and copper monolayer coated Au(111) surface, we utilized two different starting potentials for our current transient measurements. They are marked as potentials A (−0.050 V) and B (−0.430 V) in Figure 1. Point C represents a potential chosen within a broad region located in the copper OPD range. Potential step (current transient) taken from A to C allowed us to monitor copper deposition onto the bare gold surface. Using potential steps B to C, copper deposition proceeds onto the gold surface previously modified with a copper UPD monolayer.

3.1.1. Copper Deposition onto the Au(111) Electrode Surface, Previously Covered by the Copper UPD Adlayer [Potential Step B to C] (pH 4). To record current transients of copper OPD onto the Au(111) electrode surface previously covered by a copper UPD adlayer, the electrode potential was step from potential B (−0.430 V, or 33 mV more positive than the Nernst potential) to the desired potential C, in the OPD region (see Figure 1). Values for potential C were kept in the region between −0.472 and −0.489 V. Figure 2 shows the set of recorded current transients, with a typical, single-current maximum. At lower overpotentials (9−11 mV, curves a, b, and c), we observed a broad transient maximum, which became more defined at higher overpotentials. According to our analysis of the current decline in the region following the transient maximum value, the process kinetics are determined by diffusion control, which can be defined by a Cottrell equation. The estimated diffusion coefficient ($D = 7 \times 10^{-6}$ cm^2 s^{-1}) is very close to the published value.[47]

In regard to the shape of the experimental current transients, we decided to use Scharifker et al. theory[50−53] for a 3D nucleation and growth mechanism limited by a mass transfer reaction (3D-DC) to evaluate further the kinetic parameters. This theoretical approach requires presentation of current transients in a nondimensional form, plotting normalized values for current vs time [$(I/I_{max})^2$ and (t/t_{max})]. Comparison of theoretical plots for the instantaneous or progressive nucleation mechanism with the experimental transient defined the real kinetic parameters. Figure 3 shows such a nondimensional plot for typical current transients recorded at −0.477 and −0.489 V, which indicates a progressive type of nucleation. At overpotentials greater than 16−20 mV, nucleation tends to switch toward the instantaneous type. To estimate typical kinetic parameters for copper OPD deposition onto Au(111), we used Scharifker's [51,53] general eq 1 for time evolution of the current density via a 3D nucleation

$$I_{3D-DC}(t) = \left(\frac{zFD^{1/2}C}{\pi^{1/2}t^{1/2}}\right)\left(1 - \exp\left\{-N_o\pi k'D\left[t - \frac{1-\exp(-At)}{A}\right]\right\}\right) \quad (1)$$

process limited by diffusion control growth (I_{3D-DC}). This equation is equally valid for describing instantaneous and progressive nucleation and does not require classification of the nucleation mechanism, prior to use. zF is the molar charge transferred during electrodeposition, D is the diffusion coefficient, and C is the bulk concentration of the electroactive species. Time is t, the number density of active sites is N_o, the nucleation rate constant is A, and eq 2 defines k'. M and ρ are

$$k' = \frac{4}{3}\left(\frac{8\pi CM}{\rho}\right)^{1/2} \quad (2)$$

the atomic weight and the density of the deposit, respectively. Table 1 shows characteristic kinetic parameters, the nucleation rate (A), number density of active sites (N_o), and product AN_o, obtained from our experimental data using eq 1.

Quantitative analysis of the current transients indicates a 3D progressive nucleation process with diffusion-controlled growth with AN_o values very similar to those previously reported by Kolb et al.[47] for copper OPD kinetics performed under similar experimental conditions (sulfate electrolyte, pH 4, potential step B to C). Increasing the overpotential yielded higher AN_o values in both studies. However, since we used a general and more versatile equation of Scharifker et al., we also noticed that increasing the overpotential led to a change of the nucleation mechanism from progressive to instantaneous, which was not reported before.

TABLE 1: Characteristic Kinetic Parameters: (A) Nucleation Rate, (N_0) Number Density of Active Sites, and Product ANo with Total Amount of the Involved Charge (q) Obtained for Copper OPD from 1 mM $CuSO_4$ + 0.1 M H_2SO_4 (pH 4) onto the Au(111) Surface Previously Coated by a Cu UPD Adlayer, Using Eq 1

$-E$/V	η/V	t_m/s	$-I_m/\mu A\ cm^{-2}$	A/s^{-1}	$10^{-7}\ N_o/cm^{-2}$	$10^{-7}\ AN_o/s^{-1}\ cm^{-2}$	q_{total} (exp)/$\mu C\ cm^{-2}$
0.473	0.010	10.10	121	0.04	0.24	0.009	865
0.474	0.011	6.10	155	0.21	0.31	0.065	1262
0.476	0.013	3.45	198	0.40	0.44	0.176	1615
0.477	0.014	2.50	223	0.60	0.52	0.312	1766
0.479	0.016	1.70	273	1.08	0.66	0.713	1977
0.481	0.018	1.45	304	1.48	0.80	1.180	2078
0.482	0.019	1.20	331	1.50	1.00	1.500	2147
0.483	0.020	1.10	346	1.78	1.08	1.920	2186
0.484	0.021	0.95	364	2.08	1.14	2.370	2219
0.485	0.022	0.85	388	2.65	1.15	3.050	2242
0.486	0.023	0.75	406	3.25	1.21	3.930	2293
0.487	0.024	0.70	415	4.24	1.32	5.600	2337
0.488	0.025	0.65	431	6.24	1.53	9.550	2265
0.489	0.026	0.60	458	6.60	1.70	11.20	2258

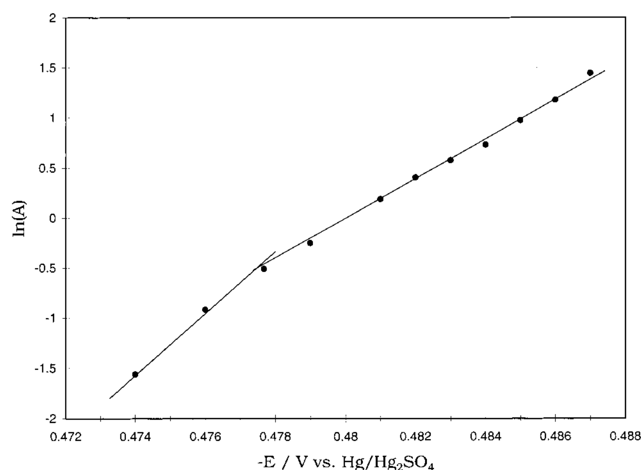

Figure 4. ln(A) (logarithm of the nucleation rate) vs the electrode potential for Cu OPD on Au(111) previously covered by a Cu UPD adlayer from 1 mM $CuSO_4$ + 0.1 M H_2SO_4 (pH 4) solution. Experimental conditions are as described in Figure 2.

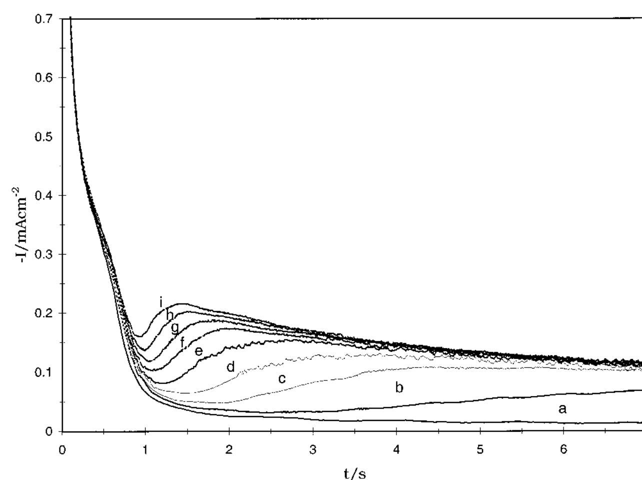

Figure 5. Set of experimental current transients recorded for copper OPD onto bare Au(111) surface from 1 mM $CuSO_4$ + 0.1 M H_2SO_4 (pH 4) solution, at different electrode potentials: (a) −0.462 V, (b) −0.470 V, (c) −0.475 V, (d) −0.480 V, (e) −0.485 V, (f) −0.490 V, (g) −0.495 V, (h) −0.500 V, (i) −0.505 V. The starting potential was −0.05 V (marked as A in Figure 1).

In addition to the previous data, we estimated the kinetic parameters of nucleation rate (A) and number density of active sites (N_o) as independent parameters. As seen in Table 1, A and N_o show potential dependence and increase with the rise of the deposition overpotential. This also supports our observation that at higher overpotentials, the nucleation tends to switch toward the instantaneous process. The slope of the ln(A) vs E (electrode potential) plot and eq 3 were used to estimate the

$$N_c = \frac{KT}{ze_0}\left(\frac{d \ln A}{dE}\right) - \beta \tag{3}$$

size of a copper critical nucleus (N_c) in the framework of the atomistic theory.[54] N_c is critical nucleus size, K is the Boltzmann constant, T is the absolute temperature, z is the number of electrons transferred during the electrochemical reaction, and β is the kinetic transfer coefficient.

Figure 4 shows a linear dependence of ln(A) vs E, in two distinct regions. At lower overpotentials, N_c (the slope of the ln(A) vs E plot) is 3, indicating that three atoms are required to form a stable nucleus. At overpotentials higher than 11 mV, the N_c value revealed a two-atom requirement. This means that, at lower overpotentials, more atoms are needed to form the critical cluster, which serves as a stable nucleus for further spontaneous growth, than at the higher overpotentials. Such a dependence of N_c on the applied overpotential is not unexpected, and has been observed before in different systems.[55−56] Interestingly, using a different approach based on the presumption that N_o is a potential-independent parameter, Kolb et al.[47] also found that N_c is 2.

3.1.2. Copper Deposition onto the Bare Au(111) Electrode Surface, with the Copper UPD Process as the Early-Stage Process [Potential Step A to C] (pH 4). Kinetic characteristics of the copper UPD process onto the copper-free Au(111) electrode surface were observed when the electrode potential was switched from potential A to potential C (see Figure 1). Potential A (−0.05 V) was in the region where Au(111) is free from copper UPD deposit. Thus, when the potential step was executed, both Cu UPD and OPD could proceed. The current transients obtained were of complex shape (Figure 5) with two or more current maxima. The most pronounced (well-defined) maximum was found in the region between 1 and 2 s. A rather broad maximum was found in the time zone 0−1 s, just after the current decrease due to double-layer, charging phenomenon. The first broad maximum (0−1 s) is associated with the copper UPD process, and the second (1 to 2 s) is associated with the copper OPD process.

Quantitative interpretation of such multimaximum transients is performed by a recently developed method[48] which we adapted combining and simulating different nucleation and growth processes (2D-2D, 2D-3D, etc.). The best description of the current transients obtained was achieved during simulation

of the following equation:

$$I = I_{DL} + I_{2Di-LI} + I_{3D-DC} \quad (4)$$

I_{DL} is the transient current due to the double charging, I_{2Di-LI} is the current contribution due to 2D instantaneous nucleation followed by the lattice incorporation process, and I_{3D-DC} is the current due to a 3D nucleation process followed by a diffusion-controlled growth.

A quantitative estimate of the double-layer charge contribution was based on a Langmuir-type adsorption−desorption equilibrium and mathematical formalism previously used by Kolb and co-workers [46] and is represented by eq 5. $k_1 = k_2 q_{ads}$, and k_1 is related to the total charge due to the adsorption process (q_{ads}).

$$I_{DL}(t) = k_1 \exp(-k_2 t) \quad (5)$$

To describe the 2D instantaneous nucleation, the model developed by Bewick, Fleischmann, and Thirsk (BFT)[57] was used. The BFT model was developed to describe a 2D growth, determined by the lattice incorporation of adatoms to the periphery of the growing nuclei and taking into account the overlap between neighboring nuclei. According to the BFT model, eq 6

$$I_{2Di-LI}(t) = \frac{2\pi zFMhN_o k_g^2 t}{\rho} \exp\left(-\frac{\pi M^2 N_o k_g^{\,2} t^2}{\rho^2}\right) \quad (6)$$

could be used to describe the current transient due to an instantaneous two-dimensional nucleation process. k_g is the lateral growth rate constant of nuclei, h is the height of the deposited layer and the other terms were defined above.

To describe the three-dimensional diffusion control process, we used the model and eq 1 proposed by Scharifker and Mostany.[51,53] In the more extended version the summary eq 4 for the cumulative current transient can be written as

$$I = k_1 \exp(-k_2 t) + p_1 t \exp(-p_2 t^2) + p_3 t^{-1/2}\left(1 - \exp\left\{-p_4\left[t - \frac{1 - \exp(-p_5 t)}{p_5}\right]\right\}\right) \quad (7)$$

where

$$p_1 = \frac{2\pi zFMhN_o k_g^{\,2}}{\rho}, \quad p_2 = \frac{\pi M^2 N_o k_g^{\,2}}{\rho^2}, \quad p_3 = \frac{zFD^{1/2}C}{\pi^{1/2}}$$

$$p_4 = N_o \pi k' D, \quad p_5 = A$$

Calculation of theoretical current transients involves nonlinear fitting of eq 7 to experimental transients, via simultaneous variation of all parameters, according to the Marquadt−Levenber algorithm.[58]

Figure 6 shows an experimental current transient (−0.490 V, η = 27 mV) with appropriate theoretical counterpart and its partial contributions. I_{2Di-LI} and I_{3D-DC} are assigned to the copper UPD and to the copper OPD, respectively. These results demonstrate that formation of 2D (UPD) copper film before OPD is an inevitable process. The OPD process is, thereby, always preceded by UPD film formation. The total charge distribution between copper UPD and OPD processes (Table 2) is also interesting. Total charge within the single transient was estimated from the experimental curve. Partial charge contributions for DL and 2Di-LI processes, both of which should be attributed to the UPD process, were estimated from the theoretical curves. The charge related to the 3D-DC process

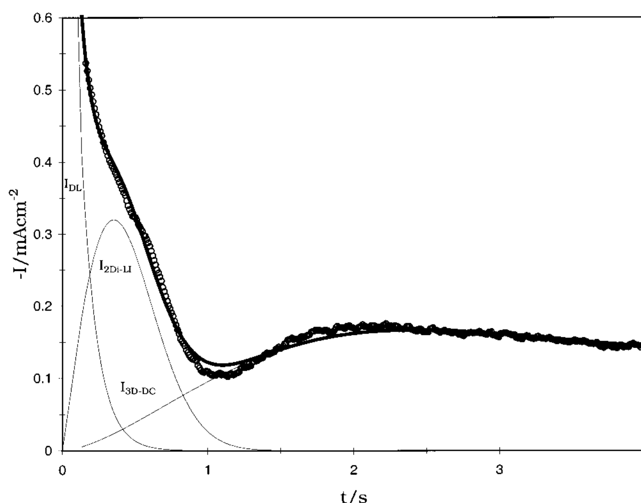

Figure 6. Comparison between the experimental current transient (○), recorded at −0.490 V, with a corresponding theoretical curve (−), for Cu deposition onto the bare Au(111) surface. Individual contributions to the theoretical current transient from the double-layer-charging phenomenon (I_{DL}) and two consecutive nucleations (I_{2Di-LI} and I_{3D-DC}, which correspond to copper UPD and OPD processes, respectively) are estimated with respect to eq 7 and presented separately. The experimental transient was recorded under conditions as described in Figure 5.

(copper OPD) was calculated as the difference between total charge and UPD contribution. As observed for the UPD process, the charge involved varied from 300 to 350 μC cm^{-2}, which is lower than expected (390 μC cm^{-2})[47] for formation of a pseudomorphic copper monolayer on the Au(111) surface at pH 4. Under our experimental conditions, the measurements showed that the OPD process started before the surface was completely covered by copper 2D-UPD film. The overlap between the UPD and OPD processes could be seen in Figure 6.

It is also interesting to compare values of the kinetic parameters for copper 3D growth in OPD in experiments carried out onto copper-free Au(111) (Table 2) and copper (UPD) covered Au(111) (Table 1). For the same overpotential of 22 mV, the copper nucleation rate (A) on the bare, copper-free, Au(111) surface is significantly lower than on copper-covered Au(111). During the first 10 s of the deposition process for most overpotentials, more charge (almost 2 times greater) passed for the copper-modified Au(111) electrode than for the copper-free gold electrode. At the same time, the number of active sites for the 3D nucleation process was found to be slightly different between these two kinds of surfaces. The copper-free Au(111) surface apparently possesses more active sites than the copper-modified surface.

The nucleation rate (A) decreased as the overpotential increased, but the number of active sites (N_o) appeared to be independent of the overpotential value. This trend is the opposite of that presented in Table 1. From AN_o values and total amount of charge involved in copper deposition, the deposition of copper onto the copper-modified Au(111) is shown to be a favorable process. This illustrates how using current transient measurements is useful for obtaining information about substrate characteristics and mechanisms which take place during the surface reaction.

To estimate copper critical nuclei size (N_c) for 3D growth, ln(A) (nucleation rate) vs E (electrode potential) was plotted in Figure 7. The values obtained for N_c were found to be 2 and 4, for the upper and lower overpotential regions, respectively.

TABLE 2: Kinetic Parameters of the Copper Deposition Process from 1 mM $CuSO_4$ + 0.1 M H_2SO_4 (pH 4) onto Bare Au(111), Estimated Using Eq 4

			I_{DL}			I_{2D-LI}		I_{3D-DC}				
$-E$/V	η/V	q_{total}(exp)/ μCcm^{-2}	$10^3 k_1$/A cm^{-2}	k_2/s^{-1}	q_{ads}(theoretical)/ μCcm^{-2}	$N_o k_g^2$/mol^2 cm^{-6} s^{-2}	q_{2Di-LI}(theoretical)/ μCcm^{-2}	$10^6 D$/cm^2 s^{-1}	A/s^{-1}	10^{-7} N_o/cm^{-2}	10^{-7} AN_o/s^{-1} cm^{-2}	q_{3D-DC}/μC cm^{-2}
0.470	0.007	466	1.3	8.1	155	0.024	159	0.2	0.260	11.0	2.860	152
0.475	0.012	1120	1.4	9.3	150	0.030	133	0.7	0.330	10.0	3.300	837
0.480	0.017	1127	1.2	7.4	157	0.020	192	7.4	0.034	2.0	0.068	844
0.485	0.022	1390	1.3	8.6	152	0.023	191	6.9	0.019	7.0	0.133	1047
0.490	0.027	1460	1.4	9.2	150	0.025	186	7.0	0.036	6.0	0.216	1124
0.495	0.032	1500	1.5	9.7	151	0.027	181	7.1	0.076	4.0	0.304	1168
0.500	0.037	1540	1.4	9.5	148	0.029	171	7.1	0.058	6.0	0.350	1208
0.505	0.042	1580	1.5	10	150	0.031	165	7.2	0.062	7.0	0.434	1248

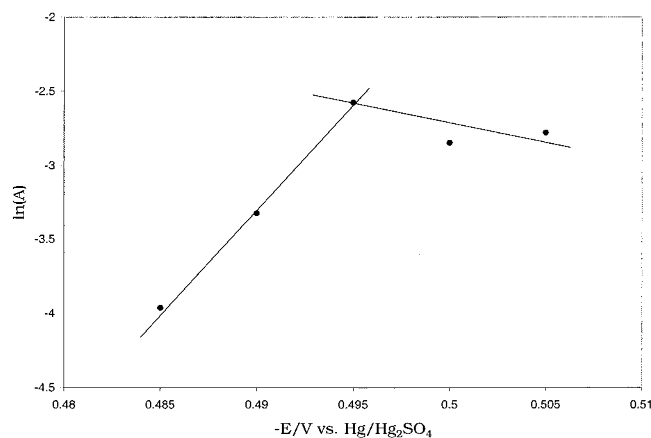

Figure 7. ln(A) (logarithm of the nucleation rate) vs the electrode potential plot for Cu OPD on bare Au(111) from 1 mM $CuSO_4$ + 0.1 M H_2SO_4 (pH 4) solution. Experimental conditions are as described in Figure 5.

These values are similar to those obtained for copper deposition onto copper-modified Au(111), suggesting the same copper−copper interactions in both cases. Consequently, differences that were observed in the copper 3D deposition kinetics should be associated with the copper−gold interactions, or the influence of UPD on the OPD process.

3.2. Copper Deposition from 0.1 M H_2SO_4 (pH 1). Figure 8 shows the typical current−potential curve for the copper UPD/OPD process onto Au(111), in 1 mM $CuSO_4$ + 0.1 M sulfuric acid (pH 1). In the voltammogram, a set of two deposition/dissolution copper UPD and OPD peaks (cathodic limit) is easily recognized. These UPD and OPD peaks are very similar to those previously reported.[2−4,6−7] Comparison to the cyclic voltammogram for the same process at pH 4 (Figure 1) demonstrates several differences. At pH 1, the UPD peaks are broader than those recorded at pH 4. The first set of deposition/dissolution peaks shifted above 50 mV toward the more negative potential. The biggest difference appeared in the second set of copper UPD peaks, which at pH 1 becomes more defined and well resolved than at pH 4. A more detailed analysis regarding the kinetics of the copper UPD process and its dependence on pH will be discussed in our future publication. In addition to changes in the UPD region, at pH 1 the copper UPD deposition peak shifted to more negative values (for 0.04 V) than at pH 4. The copper OPD dissolution peak at pH 1 also shifted toward the most positive potentials. The deposition process in a pH 1 solution is kinetically hindered (inhibited) compared to the process at pH 4, or it is simply more difficult to deposite and to dissolve copper from the Au(111) surface at pH 1 than at pH 4. These results provide clear evidence that the pH of the deposition bath indeed influences the copper UPD and OPD processes.

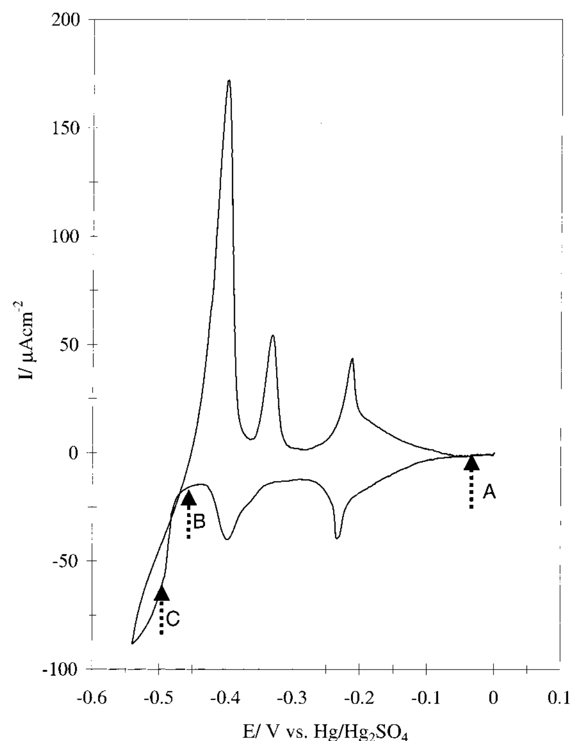

Figure 8. Cyclic voltammogram for copper deposition onto Au(111) from 1 mM $CuSO_4$ + 0.1 M H_2SO_4 (pH 1) solution. The potential scan starts at 0.0 V with a scanning rate of 15 mV/s. The voltammogram shows the copper UPD ($E > -0.463$ V) and OPD ($E < -0.463$ V) deposition regions. The marked points correspond to different initial (A and B) and final (C) potentials applied during the current transient measurement.

3.2.1. Copper Deposition onto the Bare Au(111) Electrode Surface, with the Copper UPD Process as the Early-Stage Process [Potential Step A to C] (pH 1). Figure 9 shows a set of typical current transients obtained experimentally for the copper deposition process from sulfate solution at pH 1, recorded at overpotentials of (a) 37 mV, (b) 57 mV, and (C) 137 mV, respectively. All transients possess a clear and well-defined maximum, just after step declining of the current at the beginning of the deposition process. Transient (a) possesses an additional well-defined maximum at the beginning of the deposition process (time scale less than 0.5 s). With respect to transient collection (step A to C), we believe that the first maximum, at the beginning of the deposition process, describes the copper UPD process, and the second maximum is due to the copper OPD process. To quantitatively describe the current transient which involves the double-layer-charging phenomenon and copper UPD and OPD processes, we used the same procedure and theoretical formalisms described above for interpretation of current transients presented in Figure 5. Figure 10 shows the best fit between experimental transients and

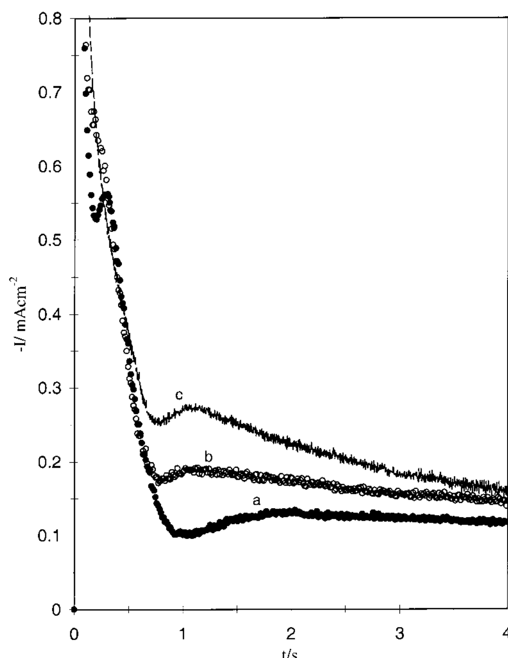

Figure 9. Set of three experimental current transients recorded for copper OPD onto the bare Au(111) surface, from 1 mM $CuSO_4$ + 0.1 M H_2SO_4 (pH 1), at different electrode potentials: (a) −0.500 V, (b) −0.520 V, and (c) −0.600 V, with a starting potential of −0.05 V (marked as A in Figure 8).

theoretical counterparts with DL, 2Di-LI, and 3D-DC processes. The first maximum, which corresponds to the copper UPD process (time scale less than 0.5 s), could be described with an instantaneous 2D nucleation process limited by lattice incorporation of copper adatoms. The copper OPD process (under the second maximum) is a 3D nucleation, mass-transfer-controlled process. It is interesting that the current transient maximum which corresponds to the copper UPD process is the most visible in the case of lower deposition overpotentials, when overlapping between 2D and 3D growth is a minimum (see Figure 10a). An increase in the copper deposition overpotential leads to higher overlapping between 2D and 3D nucleation, and the UPD maximum disappears (see Figure 10c). Parameters characteristic for copper deposition involving both UPD (2Di-LI) and OPD (3D-DC) processes estimated from quantitative analysis of these current transient are presented in Table 3. Figure 11 shows the plot ln(A) vs E, which has been used to estimate copper critical nuclei size (N_c) for the 3D-DC process. This was found to be 0 and 2, independent of the electrode potential. At higher overpotentials the 3D-DC process has a lower N_c value.

To understand the influence of pH on copper deposition on the Au(111) surface, we compared kinetic parameters derived from current transient analysis for the OPD process (3D-DC) at pH values 2 and 4 (Tables 2 and 3). Data for the kinetics of the 2Di-LI process were not compared since they were not obtained as individual parameters, but rather in the form of the $N_o k_g^2$ product. Our findings revealed the same 3D-DC mechanism for both pH values. However, some differences among kinetic parameters were observed. At pH 4 copper UPD (2Di-LI) and copper OPD (3D-DC) processes overlapped in a higher extension than at pH 1. As a result, current transients recorded a pH 1 show the position of the 2Di-LI process for copper UPD more clearly than at pH 4. The copper UPD, therefore, influences the copper OPD process less at pH 1 than at pH 4. Regarding the deposition kinetics and number of active sites for the 3D-DC process (copper OPD), the nucleation rate (A)

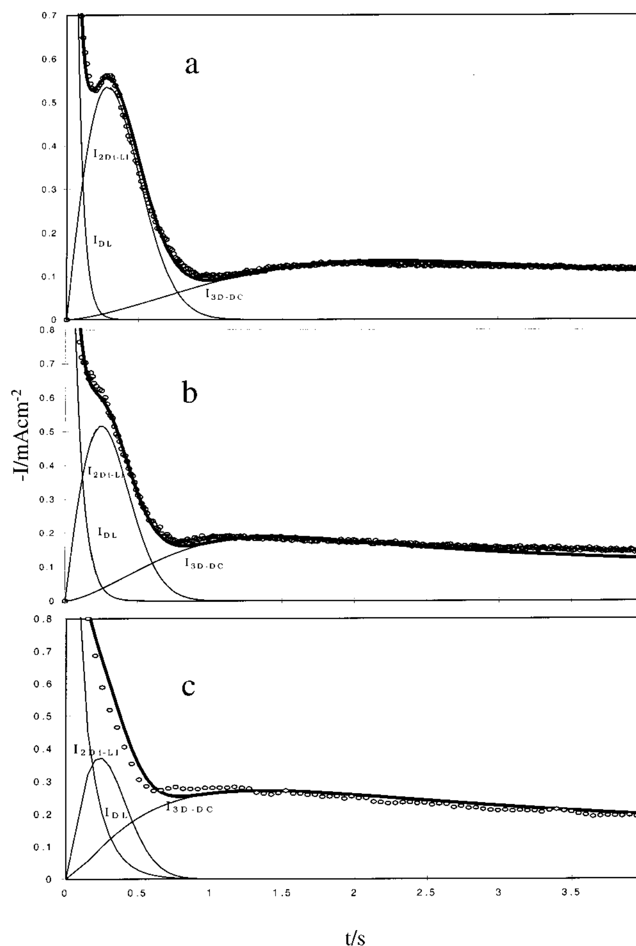

Figure 10. Comparison between experimental current transients (○) recorded at different electrode potentials, (a) −0.500 V, (b) −0.520 V, and (c) −0.600 V, with their corresponding theoretical curves (−), for Cu deposition onto the bare Au(111) surface. Individual contributions in the theoretical current transients, involving the double-layer-charging phenomenon (I_{DL}) and two consecutive nucleations (I_{2Di-LI} and I_{3D-DC}, which correspond to copper UPD and OPD processes, respectively) are estimated by means of eq 7 and presented separately. Experimental transients were recorded under conditions as described in Figure 9.

was found to be lower (nearly twice as slow) for solutions at pH 1 than at pH 4. On the other hand, the number of active sites for the copper OPD process is greater (also about twice) for the electrode surface immersed in pH 1 electrolytic solution. Both, A and N_o of the OPD process decreased at higher deposition overpotential. Apparently the UPD process plays a more significant role during deposition from pH 4 solution, providing a faster reaction rate for OPD, while lowering the number of active sites. Although our study demonstrates that the pH of the electrolytic bath influences the course of the copper deposition process, the exact mechanism and cause of this action remain obscure. In part this is due to the fact that each current transient, recorded in the regime of potential steps from A to C, describes copper deposition onto bare (UPD) and copper-modified (OPD) gold substrates, at the same time. For a comprehensive explanation of the observed findings, we require a better understanding of the solution anions' relationship to the gold substrate and copper deposit adlayer. It is well documented that the structure of the copper UPD adlayer on the Au(111) depends on the anion present and the electrode potential.[1−4,7,17,22−25] Although for some anions such as chloride, iodine, or bromine, the effect of pH could be minimal, in the case of sulfate species, which possibly exist on the gold surface

TABLE 3: Kinetic Parameters of the Copper Deposition Process from 1 mM $CuSO_4$ + 0.1 M H_2SO_4 (pH 1) onto Bare Au(111), Estimated Using Eq 4

$-E$/V	η/V	q_{total}(exp)/ μCcm^{-2}	I_{DL} 10^3k_1/A cm^{-2}	k_2/s^{-1}	q_{ads} (theoretical)/ μCcm^{-2}	I_{2D-LI} $N_ok_g^2$/mol^2 cm^{-6} s^{-2}	q_{2Di-LI} (theoretical)/ μCcm^{-2}	I_{3D-DC} 10^6D/cm^2 s^{-1}	A/s^{-1}	10^{-8} N_o/cm^{-2}	10^{-7} AN_o/s^{-1} cm^{-2}	q_{3D-DC}/μC cm^{-2}
0.500	0.037	850	4.4	24.4	180	0.0298	266	4.27	0.018	161	0.258	404
0.520	0.057	1040	2.5	16.0	157	0.0406	213	5.24	0.16	3.97	0.635	670
0.600	0.137	1260	1.5	8.0	189	0.0457	145	7.56	2	0.036	1.51	926

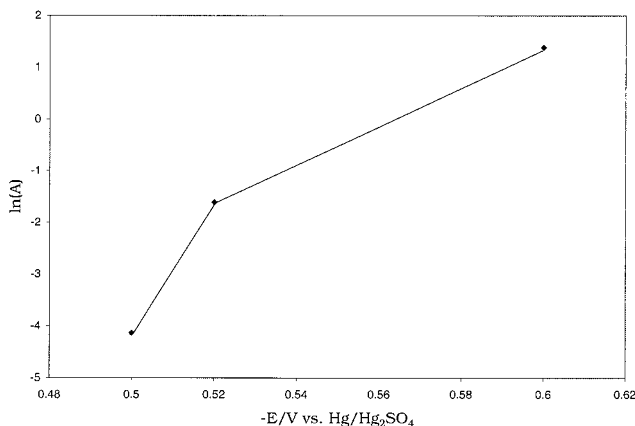

Figure 11. ln(A) (logarithm of the nucleation rate) vs the electrode potential plot, for Cu OPD on the bare Au(111) surface from 1 mM $CuSO_4$ + 0.1 M H_2SO_4 (pH 1) solution. Experimental conditions are as described in Figure 9.

as bisulfate or sulfate coadsorbed with water, changes in the pH value can have a profound influence on the copper UPD process. Few reports have evaluated the influence of pH on the copper OPD process. One reason for this is a general opinion that anions do not influence the OPD process as they do in the case of UPD. Regarding this, i.e., the weakly adsorbed, noncomplexing anions, such as sulfate or bisulfate, should not significantly influence the course of the metal OPD process. However, Kolb et al.[47] showed that depending on the electrolyte pH, copper deposition in the sulfate media could proceed via two different nucleation mechanisms: instantaneous at pH 2 and progressive at pH 4.

The results of our study demonstrate both qualitatively and quantitatively that the pH of the electrolytic bath impacts the kinetics of the copper bulk deposition process. We believe this effect it related to the presence of sulfate species at the electrode surface. Sensitivity to pH is due to the adsorption of sulfate species at the copper topmost adlayer of the copper-covered gold electrode and not to the gold substrate, itself, as in the case of the UPD process. Therefore, in the OPD region where the gold electrode is covered with one or few monolayers of copper deposit, it should be treated as a copper substrate. The copper electrode's potential of zero charge (pzc) is more negative (−0.60 V)[59] than that of the gold electrode surface (−0.140 V)[60,61] by about 0.460 V, which means that in the OPD region (limited up to −0.600 V, in our experiments), the electrode surface covered by copper UPD and OPD deposit is positively charged. In this case, adsorption of anions (sulfate species) from solution onto the electrode surface is expected to take place. In fact, the presence of sulfate species at the copper OPD adlayer over gold substrate was demonstrated in the early Auger electron spectroscopy (AES) and X-ray measurements,[1] as well in the electrochemical quartz crystal microbalance study.[20]

STM studies recently revealed the presence of organized sulfate species adlayers at the Cu(111) surface in contact with sulfuric acid electrolyte at potentials more positive than −0.75 V.[62,63] The nature of this adsorbed sulfate species (sulfate or bisulfate) has yet to be identified. Our study demonstrates the influence of pH on the copper OPD process, which we believe is related to the adsorption of different sulfate species at the copper deposit. At pH 1, the copper deposit is presumably covered with bisulfate anions, since bisulfate is the dominant species in solution. Y. Shingaya and M. Ito[64] recently claimed that bisulfate is adsorbed onto the copper substrate and the copper deposit on a Pt electrode, in 0.5 M sulfuric acid solution. At pH 4, we suppose that sulfate is the dominant species in solution and at our electrode surface. Such simple logic helps us to explain the kinetic differences found for copper deposition at different pH values. At pH 1, copper nucleation and growth during the OPD process occur much more slowly, but on a greater number of active sites, than in a pH 4 solution. Inversely, fewer available active sites, but a faster nucleation rate, were found for surfaces covered by sulfate (pH 4), which means that sulfate adsorbs more strongly to the copper deposit substrate and blocks some of the active sites. The OPD voltammetric peaks in pH 1 solution shifted toward more negative potentials, which could be due to a slower copper nucleation rate and kinetic hindrance.

However, our simplified concept is in disagreement with many already published reports, on the basis of claims that sulfate species adsorb to metal surfaces (Au, Pt, Ag, Rh) in a preferential form, i.e., sulfate or bisulfate, regardless of the dominant species in solution.[61,65−74] In general, these conclusions are based on the assumption that surface-bound anions (i.e., sulfate) possess a pK_a value different from that of anions in solution, and therefore, the adsorbed species in the adlayer is not necessarily the dominant species from solution. Considering these possibilities, the whole picture becomes even more complex, especially taking into account that different sulfate species show rather specific affinity for the gold substrate and copper adlayer deposit. However, our results do not provide evidence that such a complex scenario is necessary real. We support the indication that adsorption of bisulfate and sulfate at Au(111) electrode surface covered by copper UPD or OPD deposit occurs in a pH-dependent fashion, following the simple rule that the adsorbed species on the copper adlayer is the predominant solution species.

Conclusions

We present the kinetics for copper deposition onto the Au(111) electrode surface from 1 mM Cu^{2+} and 0.1 M H_2SO_4 solutions on the basis of current transient measurements and their interpretation using a mathematical formalism specifically developed for simulation of theoretical transients. Copper deposition was chosen as the subject of our investigation because at the Au(111) surface, it proceeds via two distinct deposition processes known as UPD and OPD. Deposition was carried out from a copper electrolytic bath of pH 4 and 2. The study was proposed to investigate and understand the role and possible influence of copper UPD on the OPD process. We also aimed to determine how such an influence is recognized in the current transient curves, as a classic measure of the kinetic behavior

for metal deposition systems. The influence of the pH of the copper electrolytic baths on the kinetics of the copper deposition onto the gold substrate was also evaluated.

To record current transients containing contributions from copper UPD and copper OPD processes, the starting potential during step potential experiments was chosen in the potential region where the gold electrode was completely free of the copper deposit. The recorded current transients for copper deposition onto the bare Au(111) surface appears to be very complex, with the unusual presence of two or more current maxima. A new method for evaluation of current transients with several nucleation (deposition) processes, recently developed in our laboratory, was used for the quantitative interpretation. Our results show that, within a single current transient, kinetic contributions for UPD and OPD processes can be easily resolved and evaluated quantitatively. Unlike the classical method of recording current transients by initiating potential steps from potential regions after completion of the UPD process and focusing exclusively on OPD changes, we secured additional information to document interconnection of the UPD and OPD processes. We demonstrated that UPD could be treated as the early stage of the copper bulk deposition process. Regardless of the applied potentials, the recorded current transients showed that UPD was an inevitable process, always taking place prior to OPD deposition. To estimate how our method (initial point: the bare Au(111) surface) differs from the classical current transient measurement (initial point: the copper UPD deposit-covered Au(111) surface), we performed both types of experiments. The results obtained demonstrate that copper OPD (as a focus of comparison) can be characterized as a 3D nucleation process limited by diffusion-controlled growth (3D-DC) by both methods. Although both methods indicate the progressive type of nucleation for copper deposit during the OPD process, we noticed that, at higher deposition overpotentials, copper nucleation tends to switch to the instantaneous type. For the classic approach, an excellent correlation with previous literature data was obtained. The major advantage of our approach was the convenience of observing the contribution from the 2D (instantaneous) nucleation and growth limited by a lattice incorporation process, related to the copper UPD deposition in the recorded transients.

A detailed analysis of the major kinetic parameters for 3D-DC (OPD process) using nucleation rate (A), number density of active sites (N_o), and size of a copper critical nucleus (N_c) indicated further differences between the estimation methods. At the same overpotential (22 mV), the copper nucleation rate (A) on the bare (copper-free) Au(111) surface was lower than on the Au(111) surface covered with a copper UPD adlayer. The resulting difference in deposition kinetics showed that, during the first 10 s of the deposition process, more than twice the charge passed in the case of copper-modified Au(111) than the copper-free electrode. At the same time, no significant difference was found between the number of active sites for the 3D-DC (OPD) nucleation process for these two surfaces. Apparently, after completion of the UPD process, the 3D-DC (OPD) deposition becomes faster and even the newly created adlayer possesses fewer active sites. All these experiments, during the first phase of our investigation, were carried out from a sulfuric acid electrolyte bath at pH 4.

To evaluate the influence of the electrolytic bath (i.e., sulfate vs bisulfate) on the kinetics of copper deposition, we also performed current transient evaluation in a solution at pH 1. All transients obtained in this second part of our research were initiated on a bare Au(111) surface. The potential step was designed in this way so that, at the beginning of transient recording, the electrode surface would be completely free of the copper deposit. The current transients before obtained indicated the presence of a 2D-LI process for the copper UPD deposition and 3D-DC for the copper OPD process. The same processes were identified for both pH values. Considering the influence of UPD on the copper OPD process, at pH 4, the copper UPD (2Di-LI) and copper OPD (3D-DC) overlap extended at higher rate than at pH 1. As a result, current transients recorded at pH 1 show the position of the 2Di-LI process for copper UPD more clearly, indicating that, at this pH, the copper UPD has less influence on the copper OPD process. In terms of deposition kinetics and the number of active sites for the 3D-DC (copper OPD) process, the nucleation rate (A) is lower (twice as slow) for solutions of pH 1. However, the number of active sites for the copper OPD process is greater (about twice) for the electrode surface immersed in the pH 1 electrolytic solution. These data suggest that, during deposition from the pH 4 solution, the UPD process plays a significant role, providing a faster reaction rate for the OPD process, but lowering the number of active sites. We suppose that copper deposition is influenced by sulfate/bisulfate interaction with the copper UPD/OPD adlayer formed at the Au(111) substrate. Thus, as recently reported, the newly formed copper deposit adlayer (in the UPD and OPD potential regions) could be easily covered by sulfate species (sulfate or bisulfate). In the case of the copper UPD adlayer, an epitaxial monolayer of copper adatoms over the Au(111) substrate is considered to be formed at the end of the UPD process. Assuming that the anion species adsorbed at the electrode surface is actually equal to the dominant anion form in solution, the differences noticed in our study between the kinetics of the deposition processes carried out in electrolytic solutions with different pH values can be interpreted as following. At pH 1, when the copper deposit is presumably covered by bisulfate, copper nucleation and growth during OPD proceed much more slowly, but on a greater number of active sites. Fewer active sites, but a faster nucleation rate, were found for copper surfaces covered by sulfate, at pH 4. This allows us to conclude that sulfate adsorbs more strongly than bisulfate at the copper deposit and blocks some of the deposition active sites.

The data presented here clearly show that the UPD and OPD copper deposition processes onto the Au(111) surface are pH-dependent, and controlled by anions present on the electrode surface.

Acknowledgment. Financial assistance was received from CONACYT (Projects 0913E-P and 32158E; Catedra Patrimonial de Excelencia Nivel II and Project L0081-E9608 for N.B.). M.P.-P. acknowledges CONACYT for scholarship support and Project 32158-E.

References and Notes

(1) Zei, M. S.; Qiao, G.; Lehmpfuhl, G.; Kolb, D. M. *Ber. Bunsen-Ges. Phys. Chem.* **1987**, *91*, 349.

(2) Kolb, D. M. *Schering Lecture's Publications*; Schering Reseach Foundation, Berlin, 1991; Vol. 2, p 1.

(3) Magnussen, O. M.; Hotlos, J.; Nichols, R. J.; Kolb, D. M.; Behm, R. J. *Phys. Rev. Lett.* **1990**, *64*, 2929.

(4) Magnussen, O. M.; Hotlos, J.; Beitel, G.; Kolb, D. M.; Behm, R. J. *J. Vac. Sci. Technol.* **1991**, *B9*, 969.

(5) Manne, S.; Hanma, P. K.; Massie, J.; Elings, V. B.; Gewirth, A. A. *Science* **1991**, *251*, 183.

(6) Hachiya, T.; Honbo, H.; Itaya, K. *J. Electroanal. Chem.* **1991**, *315*, 275.

(7) Batina, N.; Will, T.; Kolb, D. *Faraday Discuss.* **1992**, *94*, 93.

(8) Haiss, W.; Lackey, D.; Sass, J. K.; Mayer, H.; Nichols, R. J. *Chem. Phys. Lett.* **1992**, *200*, 343.
(9) Ikemiya, N.; Miyaoka, S.; Hara, S. *Surf. Sci.* **1994**, *311*, L641.
(10) Hotlos, J.; Magnussen, O. M.; Behm, R. J. *Surf. Sci.* **1995**, *335*, 129.
(11) Haiss, W.; Sass, J. K. *J. Electroanal. Chem.* **1996**, *410*, 119.
(12) Nishizawa, T.; Nakada, T.; Kinoshita, Y.; Miyashita, S.; Sazaki, G.; Komatsu, H. *Surf. Sci.* **1996**, *367*, L73.
(13) Cavalleri, O.; Gilbert, S. E.; Kern, K. *Surf. Sci.* **1997**, *377–379*, 931.
(14) Tadjeddine, A.; Guay, D.; Ladouceur, M.; Tourillon, G. *Phys. Rev. Lett.* **1991**, *66*, 2235.
(15) Toney, M. F. Howard, J. N.; Richter, J.; Borges, G. L.; Gordon II, J. G.; Melroy, O. R.; Yee, D.; Sorensen, L. B. *Phys. Rev. Lett.* **1995**, *75*, 4472.
(16) Gordon, J. G.; Melroy, O. R.; Toney, M. F. *Electrochim. Acta* **1995**, *40*, 3.
(17) Wu, S.; Lipkowski, J.; Tyliszezak, T.; Hitchock, A. P. *Prog. Surf. Sci.* **1995**, *50*, 227.
(18) Chabala, E. D.; Cairns, J.; Rayment, T. *J. Electroanal. Chem.* **1996**, *412*, 77.
(19) Herrero, E.; Glazier, S.; Buller, L. J.; H. D. Abruña, *J. Electroanal. Chem.* **1999**, *461*, 121.
(20) Borges, G. L.; Kanazawa, K. K.; Gordon, J. G., II. *J. Electroanal. Chem.* **1994**, *364*, 281.
(21) Uchida, H.; Hiei, M.; Watanabe, M. *J. Electroanal. Chem.* **1998**, *452*, 97.
(22) Shi, Z.; Lipkowski, J. *J. Electroanal. Chem.* **1994**, *364*, 289.
(23) Shi, Z.; Lipkowski, J. *J. Electroanal. Chem.* **1994**, *365*, 303.
(24) Z. Shi Wu, S.; Lipkowski, J. *Electrochim. Acta* **1995**, *40*, 9.
(25) Z. Shi Wu, S.; Lipkowski, J. *J. Electroanal. Chem.* **1995**, *384*, 171.
(26) Nichols, R. J.; Kolb, D. M.; Behm, R. J. *J. Electroanal. Chem.* **1991**, *313*, 109.
(27) Nichols, R. J.; Beckmann, W.; Meyer, H.; Batina, N.; Kolb, D. M. *J. Electroanal. Chem.* **1992**, *330*, 381.
(28) Nichols, R. J.; Schroer, D.; Meyer, H. *Scanning* **1993**, *15*, 266.
(29) Stimming, U.; Vogel, R.; Kolb ant T Will, D. M. *Power Sources* **1993**, *43–44*, 169.
(30) Ullmann, R.; Will, T.; Kolb, D. M. *Chem. Phys. Lett.* **1993**, *209*, 238.
(31) Nichols, R. J.; Bach, C. E.; Meyer, H. *Ber. Bunsen-Ges. Phys. Chem.* **1993**, *97*, 1012.
(32) Nichols, R. J.; Bunge, E.; Meyer, H.; Baumgartel, H. *Surf. Sci.* **1995**, *335*, 110.
(33) Ullmann, R.; Will, T.; Kolb, D. M. *Ber. Bunsen-Ges. Phys. Chem.* **1995**, *99*, 1414.
(34) Holzle, M. H.; Zwing, V.; Kolb, D. M. *Electrochim. Acta* **1995**, *40*, 1237.
(35) Will, T.; Dietterle, M.; Kolb, D. M. The Initial Stages of Electrolytic Copper Deposition: An Atomistic View. In *Nanoscale Probes of the Solid/Liquid Interface*; Gewirth, A. A., Siegenthaler, H., Eds.; NATO ASI; Kluwer: Dordrecht, 1995; Vol. 288, p 37.
(36) Nichols, R. J. Scanning Probe Microscopy Studies of Copper Electrodeposition. In *Nanoscale Probes of the Solid/Liquid Interface*; Gewirth, A. A., Siegenthaler, H., Eds.; NATO ASI; Kluwer: Dordrecht, 1995; Vol. 288, p 163.
(37) Schmidt, W. U.; Alkire, R. C.; Gewirth, A. A. *J. Electrochem. Soc.* **1996**, *143*, 3122.
(38) Gewirth, A. A.; Niece, B. K. Electrochemical Applications of in Situ Scanning Probe Microscopy. *Chem. Rev.* **1997**, *97* (4), 1129.
(39) Eliadis, E. D.; Nuzzo, R. G.; Gewirth, A. A.; Alkire, R. C. *J. Electrochem. Soc.* **1997**, *144*, 96.
(40) Cavalleri, O.; Gilbert, S. E.; Kern, K. *Chem. Phys. Lett.* **1997**, *269*, 479.
(41) Kolb, D. M.; Ullmann, R.; Will, T. *Science* **1997**, *275*, 1097.
(42) Eliadis, E. D.; Alkire, R. C. *J. Electrochem. Soc.* **1998**, *145*, 1218.
(43) Kolb, D. M.; Schneeweiss, M. A. The Electrochemical Society, INTERFACE, 1999, 8 (1) 26.
(44) Nichols, R. J. Imaging Metal Electrochristallization at High Resolution. In *Imaging of Surfaces and Interfaces (Frontiers of Electrochemistry, Vol. 5)* Lipkowski, J., Ross, P. N., Eds. Wiley-VCH, Inc, 1999, p 99.
(45) Xia, X. H. Schuster, R.; Kirchner, V.; Ertl, G. *J. Electroanal. Chem.* **1999**, *461*, 102.
(46) Holzle, M. H.; Retter, U.; Kolb, D. M. *J. Electroanal. Chem.* **1994**, *371*, 101.
(47) Holzle, M. H.; Apsel, C. W.; Will, T.; Kolb, D. M. *J. Electrochem. Soc.* **1995**, *142*, 3741.
(48) Palomar-Pardavé, M.; Miranda-Hernández, M.; González, I.; Batina, N. *Surf. Sci.* **1998**, *399*, 80.
(49) Palomar-Pardavé, M. E. Ph.D. Thesis, Universidad Autónoma Metropolitana-Iztapalapa, México, 1998.
(50) Scharifker, B. R.; Hills, G. *Electrochim. Acta* **1983**, *7*, 879.
(51) Scharifker, B. R.; Mostany, J. *J. Electroanal. Chem.* **1984**, *177*, 13.
(52) Palomar-Pardavé, M.; Ramírez, M. T.; González, I.; Serruya, A.; Scharifker, B. *J. Electrochem. Soc.* **1996**, *143*, 1539.
(53) Scharifker, B. R.; Mostany, J.; Palomar-Pardavé, M.; González, I. *J. Electrochem. Soc.* **1999**, *14*, 1011.
(54) Milchev, A. Stoyanov, S.; Kaichev, R. *Thin Solid Films* **1974**, *22*, 267.
(55) Milchev, A.; Vassileva, E.; Kertov, V. J. *Electroanal. Chem.* **1998**, *107*, 323.
(56) Serruya, A.; Mostany, J.; Scharifker, B. R. *J. Chem. Soc., Faraday Trans.* **1993**, *89*, 255.
(57) Bewick, A.; Fleischmann, M.; Thirsk, H. R. *Faraday Soc.* **1962**, *58*, 2200.
(58) Burden, R. L.; Faries, J. D. *Numerical Analysis*, 4th ed.; PWS-Kent: Boston, 1989.
(59) Bertocci, U.; Turner, D. R. In *Encyclopedia of Electrochemistry of the Elements*; Bard, A. J., Ed.; Marcel Dekker: New York, 1974; Vol. II, Chapter 6.
(60) Shi, Z.; Lipkowski, J.; Gamboa, M.; Zelenay, P.; Wieckowski, A. *J. Electroanal. Chem.* **1994**, *366*, 317.
(61) Ataka, K.; Osawa, M. *Langmuir* **1998**, *14*, 951.
(62) Wilms, M.; Broekmann, P.; Stuhlmann, C.; Wandelt, K. *Surf. Sci.* **1998**, *402–404*, 88.
(63) Hu Li, W.; Nichols, R. J. *J. Electroanal. Chem.* **1998**, *456*, 153.
(64) Shingaya, Y.; Ito, M. *J. Electroanal. Chem.* **1999**, *467*, 299.
(65) Zei, M. S.; Scherson, D.; Lehmpfuhl, G.; Kolb, D. M. *J. Electroanal. Chem.* **1987**, *229*, 99.
(66) Magnussen, O. M.; Hageb`ck, J.; Hotlos, J.; Behm, R. J. *Faraday Discuss.* **1992**, *94*, 329.
(67) Shi, Z.; Lipkowski, J.; Gamboa, M.; Zelenay, P.; Wieckowski, A. *J. Electroanal. Chem.* **1994**, *366*, 317.
(68) Edens, G. J.; Gao, X.; Weaver, M. J. *J. Electroanal. Chem.* **1994**, *375*, 357.
(69) Mrozek, P.; Han, M.; Sung, Y. E.; Wieckowski, A. *Surf. Sci.* **1994**, *319*, 21.
(70) Funtikov, A. M.;, Stimming, U.; Vogel, R. *Surf. Sci. Lett.* **1995**, *324*, 343.
(71) Wan, L. J.; Yau, S. L.; Itaya, K. *J. Phys. Chem.* **1995**, *99*, 9507.
(72) Nishizawa, T.; Nakada, T.; Kinoshita, Y.; Miyashita, S.; Sazaki, G.; Komatsu, H. *Surf. Sci. Lett.* **1996**, *367*, 73.
(73) Funtikov, A. M.;, Stimming, U.; Vogel, R. *J. Electroanal. Chem.* **1997**, *428*, 147.
(74) Shingaya, Y.; Ito, M. *J. Electroanal. Chem.* **1999**, *467*, 299.